

Fourth European Rotorcraft and Power Lift
Aircraft Forum

Paper No. 15

Hot Wire Measurements of Stall
and Separation on Helicopter Rotor Blades*

H. R. Velkoff

R. L. Ghai

Department of Mechanical Engineering

The Ohio State University
Columbus, Ohio
U.S.A.

September 13-15, 1978

Associazione Italiana di Aeronautica ed Astronautica

Associazione Industrie Aerospaziali

HOT WIRE MEASUREMENTS OF STALL AND SEPARATION ON HELICOPTER ROTOR BLADES

H. R. Velkoff and R. L. Ghai
Ohio State University
Columbus, Ohio, U.S.A.

1. INTRODUCTION

The demand for increased productivity of helicopters has brought an increasing attention to their aerodynamic characteristics. A major limitation to increasing helicopter speed arises from retreating blade stall. Though blade stall has been the object of concern and study for many years, only relatively recently have extended efforts been made to understand it more fully or to mitigate its effects. Studies of flow separation on airfoils and measurements of boundary layers have been made and new airfoils, configured to further enhance C_L , have been developed.

The penalties imposed by stall of the retreating blade arise in the form of increased power requirements, high control forces, and aircraft vibration. For typical airfoil sections used on helicopters one can expect either leading edge or trailing edge stall to occur. The type of stall that occurs can greatly affect the characteristics of the resulting loss of lift.

Three basic types of stall have been identified; i.e., trailing edge stall, leading edge stall, and thin airfoil stall. They have been discussed by Lachmann¹ and others.

The stalling process has also been associated with the formation and shedding of a vortex from the leading edge. When this happens flow circulation is lost. Since airfoil lift depends on the circulation, the lift decreases and the blade becomes stalled. Experimental evidence of vortex shedding has been obtained by McCroskey².

It is evident that the phenomenon of blade stall is closely related to boundary layer effects. The boundary layer profile for an NACA 0012 airfoil was experimentally determined using hot wire anemometry in a study done by Velkoff, Hoffman, and Blaser³. The data verified the existence of laminar separation bubbles with reattachment between 20 and 25 percent chord for a Reynolds number of 158,000 and 10° pitch. Evidence of separation bubbles was also indicated by ammonia trace studies done by Velkoff, Blaser, and Jones⁴.

McCroskey² has studied the nature of stall on helicopter airfoils extensively in two-dimensional wind tunnel tests but studies of separation were not made on rotors in forward flight. The measurements made by Velkoff et al³ determined boundary layer characteristics in hovering and in forward flight, but no studies were made of the pattern of stall formation and propagation. The purpose of this work is to examine the stall propagation on a rotor at various advance ratios.

2. APPROACH

The nature of rotor blade stall during hover and simulated forward flight was studied through tests conducted on a rotating model rotor blade installed in a flow channel. The investigation was entirely experimental using hot wire anemometry techniques. The data obtained were studied to determine the direction of the stall progression; that is, whether the stall progresses from the leading edge as with sharp leading edge airfoils, or from the trailing edge forward.

Hot wire instrumentation was used to measure the air velocity above the blade simultaneously at several positions along the chord, and continuous traces of the velocity fluctuations were obtained as a function of time. Data were taken at three selected advance ratios, blade pitch angles, and shaft angles.

The hot wire probes were installed at a height near the edge of the boundary layer; thus flow separation could be detected as a drop in the velocity at a particular hot wire location. By comparing the output of hot wires at different chordwise positions, the progression of the flow separation across the blade could be studied.

The tests were conducted at the Department of Mechanical Engineering, The Ohio State University, utilizing an existing rotor wind tunnel, an existing rotor blade, and existing hot wire measuring equipment. Hot wires were calibrated prior to runs to ensure the accuracy of the readings obtained.

3. EXPERIMENTAL EQUIPMENT

3.1 Flow Channel

The flow channel used during the experimental program is shown in Figure 1. It has a test section 4 feet high, 8 feet wide, and 8 feet long. Powered by a 150 hp ac motor, it is capable of air speeds of 100 fps through the test section. A set of variable vanes control the flow velocity which was measured with a pitot tube to within ± 3 fps. A thorough description of this flow channel is presented by Velkoff et al.⁴.

3.2 Rotor Blade and Drive System

A single-bladed NACA 0012 model rotor was used for the tests. The blade and drive system are shown in Figure 2. It has a 41-3/4-inch radius and a 9-inch chord. The blade pitch angle could be adjusted at the hub. A hinged connection between the blade hub and the drive shaft allowed the blade to flap freely.

The rotor was powered by a 10 hp air motor connected to a 100 psi supply line. The rotor speed could be controlled by a valve which regulates the air flow rate to the motor. The motor, belt drive assembly, and drive shaft tilted as a unit by adjusting a lead screw. This allowed variation of the drive shaft angle. Cables from the instrumentation on the hub were fed through the center of the hollow drive shaft to a slip ring unit at the base of the shaft.

Maintaining a constant rpm required frequent adjustments to the valve regulating the air flow rate to the motor. It is estimated that the desired rotor speed was maintained within ± 3 rpm. The blade pitch angle and shaft angle settings were accurate to $\pm 0.5^\circ$.

3.3 Hot Wire Instrumentation

The air velocity above the blade surface was measured with constant-temperature hot wire anemometers. The hot wires and anemometers are described in reference 3. Since flow data at several locations were required simultaneously, three hot wire probes with three separate anemometer circuits were used. Their output was recorded on light-sensitive paper. The probes were installed on the rotor at a radius of 33-1/2 inches, and the wire leads were fed through the inside of the blade. Three hot wires were used to take simultaneous readings but their locations were shifted during the tests to provide velocity data at four positions on the chord.

Probe holders were designed to mount the hot wires to the blade and measured approximately 1 inch on each side, and the probes extended 2-1/2 inches from the holders toward the blade tip. The probe holders did not cause distortion of the probe data except for a region in the downwind position of the blade. This localized distortion can be observed in the traces taken. The probe height above the blade could be adjusted by means of a screw on the holder. A transversing microscope described in reference 3 allowed the height to be set to within ± 0.001 inch. All the tests were run at 0.040 inch above the blade.

The signals from the hot wires mounted on the blade were amplified before passing through the slip ring unit. This was necessary to prevent slip ring noise from masking the hot wire signals. The amplifiers were mounted on the rotor hub. The electric cables from the amplifier were fed through the hollow drive shaft to the slip ring unit mounted at the bottom of the drive shaft. Wires connected to the stationary part of the slip ring unit were routed to the instrument console.

To make the sensitivity of the hot wires nearly uniform linearizers were incorporated in the circuit so that the voltage output from each linearizer was a linear function of the velocity at the probe.

The linearized output of each hot wire was passed through a 150 Hz low-pass filter to make the traces easier to read without loss of the important stall information. The data were recorded using a multichannel light beam oscillograph. Along with the three hot wire velocities, the azimuth pulse from an electromagnetic transducer used to measure rotor speed was also traced on the chart.

3.4 Hot Wire Calibration System

The hot wires were calibrated using a nozzle calibration facility which provided a uniform air flow of known magnitude. It consisted of a cylindrical chamber connected to a 100 psi supply line, a conical nozzle, a valve that controlled the supply flow rate into the chamber. The nozzle velocity was known as a function of chamber pressure to within 0.5%. For a thorough discussion of the hot wire calibration device, see reference 3.

It is believed that the main source of error in velocity determination was introduced in linearizing the anemometer output before it was traced on the oscillograph chart. The reason is that the hot wire calibration curve could not be accurately linearized over the wide range of velocities encountered during the tests. For the tests reported herein the linearizers were adjusted to give the most accurate linearization over a range of 30 to 150 fps.

It is estimated that over the range of 30 to 150 fps, the recorded velocity traces represent the actual air velocity at the sensor to within ± 5 fps. From 30 fps to almost 0 fps the traces are about 2 fps higher to about 8 fps lower than the true air velocity. When the velocity at the hot wire is nearly zero, the traces indicate negative velocities and these values are believed to be attributed to the linearizer problems just discussed.

Though the absolute magnitudes of the low velocities are uncertain, in the study of blade stall it is necessary to detect large scale effects rather than to take precise velocity measurements, and hence the results obtained are considered to be quite meaningful.

4. EXPERIMENTAL PROCEDURE

The experimental program under which the final data were taken used three hot wires on the blade. For trailing edge flow study, two hot wires were mounted at the trailing edge at 54% and 71% chord locations. A third hot wire located at 10% chord was used to detect leading edge separation and was active for all tests.

The drive shaft tilt angle was set at 5°, and data were taken at blade pitch angles of 5°, 10°, and 15° with the rotor turning at 300 rpm. At each pitch angle the tunnel velocity was controlled to obtain advance ratios of 0, 0.16, 0.24, and 0.32. The rotor was stopped only to change pitch angle. The entire procedure was repeated for a shaft angle of 10°.

In order to study the progression of separation at the leading edge, the hot wire at 54% chord was moved to 24% chord. The hot wire near the trailing edge at 71% chord was left in position so that trailing edge stall could be detected. The above sequence of tests was then repeated to provide velocity data simultaneously at 10, 24, and 71% chord.

The above test program yielded data at a total of four chordwise locations. There was a fifth position available on the blade, since the original experimental program which used the switching relay employed five hot wires. Data were to have been taken at 10, 24, and 35% chord positions. The final tests did not use the relay system, and because of a lack of time no data were taken at the 35% chord position.

The hot wires were calibrated before the data were taken. During the course of the tests, which lasted about six hours, two hot wires were burned. They were replaced with other hot wires that had previously been calibrated. Two of the linearizers were then readjusted to match the calibration curve of the new hot wires.

5. RESULTS

The data are presented in the form of oscillograph traces of the hot wire outputs. Each chart is a record of the voltage output of three hot wires at different locations across the blade chord traced simultaneously. The vertical scale represents the tangential velocity components (7 fps per division) at each hot wire location, while the horizontal axis is time increasing toward the right (0.01 sec per division). The azimuth for each trace is shown at 0°, 90°, 180°, and 270°. The top chart on each page presents data taken at 10, 24, and 71% chord, and the bottom chart gives the velocities at 10, 54, and 71% chord.

Data were taken during simulated forward flight for different advance ratios, blade pitch angles, and shaft angles. The rotor speed was maintained at 300 rpm. The four hot wires were located at 81% of the blade radius at a height of 0.04 inch. The output of each wire was passed through a 150 Hz low-pass filter before being recorded on the charts. The unfiltered traces contained high-frequency components. Since the purpose of the tests was to study gross blade stall behavior rather than the high-frequency content, the charts were made easier to read by filtering out the high frequencies.

Superimposed on each hot wire trace is the free-stream velocity calculated by the formula

$$U_{\infty} = \Omega r + V \sin\psi,$$

where Ωr is the rotor speed at radius of the hot wires, V is the tunnel velocity, and ψ is the azimuth angle. These lines were added to the charts after the data had been taken to aid in interpreting the results. Also added afterward were dotted horizontal lines indicating the zero velocity axis for each hot wire.

On the forward flight data charts, the area around 0° azimuth has been cross-hatched. The validity of the data in this region is questionable because of obstruction of the flow to the hot wires by the probe holders and the hub instrumentation.

At the top and bottom edges of the charts is the recorded voltage output of the electromagnetic transducer which was activated by the rotation of the rotor shaft. It was used to locate the azimuth angles. The angles labeled on the hover data represent the blade orientation with respect to the flow channel.

It should be noted that points of equivalent azimuth angles do not lie on a vertical line. At every instant of time, each hot wire is at a different azimuth angle corresponding to its position on the chord. Since the free-stream velocity line for each hot wire location was plotted as a function of azimuth angle, it too is shifted along with the azimuth angle.

There are some places in the charts where a hot wire trace dips slightly below the zero velocity axis associated with it. This is a consequence of inaccuracies at very low velocities introduced by linearizing the hot wire output, as previously discussed. It does not indicate a negative velocity. In fact the hot wires cannot be used to distinguish reverse from forward flow since their output is always positive regardless of the velocity direction. However this fact does not lead to any ambiguities in interpreting the recorded data.

In some instances it is of interest to determine the velocity at which a fluctuation in the flow sweeps across the blade. Some portions of the traces showing a correspondence between the output of two hot wires have been connected by dotted lines. The horizontal shift represents the time required to travel the distance between the two hot wire locations. Since the distance is known, the velocity with respect to the blade can be calculated, and it is nondimensionalized by dividing it by a representative velocity taken as the average of the theoretical free stream velocities at each end of the dotted line. Thus the velocities relative to the blade are given as a fraction of the free stream velocity.

6. ANALYSIS AND INTERPRETATION

6.1 General Evaluation

The significant data for this study were taken under conditions simulating forward flight where retreating blade stall was observed. Many traces, as will be seen, show the hot wire output dropping off and departing from the shape of the free-stream velocity curve, indicating separation. When it occurs near the leading edge, the stall appears to be distinctly different from that at the trailing edge.

While little difference was noted in general between the data taken at shaft tilt angles of 5° and 10° , the blade pitch angle is a significant parameter regarding the magnitude and nature of the stall. At pitch angles of 10° and less there is separation only near the trailing edge at the 54 and 71% chord locations.

The stall onset and recovery is very gradual, and the separation point seems to move from the trailing edge forward up to a certain point, then back again. Some traces at low pitch angle, figures 3 and 4, show definite separation at 71% chord with little or no separation at 54% indicating that the stall does indeed originate at the trailing edge. These characteristics are typical of trailing edge stall.

For increasing pitch angles and advance ratios, the stall increases in magnitude and spreads to encompass a large segment of the cycle. The center of the stall region appears to be delayed in that instead of occurring at an azimuth angle of 270° when the free-stream velocity is lowest, it is generally centered around an angle of about 340° . The stall usually seems to initiate at angles ranging from about 240° to 300° .

Because of the erratic, turbulent nature of the trace patterns and the gradual onset of the trailing edge stall, the azimuth angle that the flow becomes separated cannot be exactly determined. However, for some of the charts at low pitch angles this point can be estimated. It is then possible to approximately calculate the velocity that the separation sweeps across the blade during trailing edge stall onset and recovery. The values range from about 3 to 9% of the theoretical free stream velocity for mild stalls as shown in figures 4, 5, 7, 9, 10, 11, and 12.

At the highest pitch angles, separation at the leading edge occurs along with the trailing edge stall, and it has quite different characteristics from trailing edge stall. The onset and recovery is abrupt with very rapid progression across the blade.

It is difficult to accurately determine the velocity with which the stall sweeps back from the leading edge since the point at which separation occurs can only be estimated. However, it is clear that the rate of progression is much higher than that at the trailing edge, and it approaches the free-stream velocity in magnitude.

Although the direction of progression is difficult to determine in some of the charts, the top charts in figures 16 and 18 seem to show that the stall progresses rearward at the onset and back toward the leading edge upon recovery.

One possibility is that the rearward progression of the stall onset may be caused by the growth of a long bubble as in thin airfoil stall. If this were the case the bubble growth would be gradual as the blade loading changes.

However, the data indicate that the progression is not at all gradual. Rather, the separation sweeps across the blade very suddenly as if a short bubble were bursting. Therefore, the stall seems to be a type of leading edge stall rather than thin airfoil stall.

This suggests that a small laminar separation bubble may exist somewhere upstream of the hot wire at 10% chord. As the angle of attack increases critical blade loading may be reached, the bubble suddenly bursts, and the disturbance is swept downstream.

The top chart shown in Figure 15 is of particular interest. It shows evidence of separation at 10% chord with attached flow at 24% chord and severe stall at the trailing edge. This indicates that the leading edge separation is indeed a separate phenomenon from stall at the trailing edge, and it originates

at the leading edge. The separation occurring at 10% chord suggests the presence of a laminar separation bubble with reattachment somewhere between 10 and 24% chord or the influence of the separation bubble may not have swept rearwards yet. The flow apparently separates near the trailing edge independent from the leading edge separation.

Flow attachment or reattachment in midchord, such as that shown in Figure 15, was not observed during leading edge stall in the traces of other conditions. This observation may have been a rare occurrence caused by the rapidly changing angle of attack from blade flapping or flow field non-uniformity. Rapid changes in blade loading can induce abnormal pressure gradients along the chord causing unusual boundary layer behavior.

Another possible explanation for the reattachment shown in Figure 15 is that it shows the formation of a long bubble which does not grow past the 24% chord location. This would imply thin airfoil stall; however, this is probably not the case since none of the other charts seem to indicate long bubble formation. They show a very sudden stall progression as if a short bubble were bursting.

Apart from the stall phenomenon, in some instances small individual disturbances in the flow can be traced as they sweep rearward across the blade. They show up as a correspondence in the shape of two hot wire outputs. The rate of progression across the blade was calculated for some of these and are labeled on the charts. The velocities ranged from 30 to 100% of the free-stream velocity. These disturbances may be fluctuations in the potential flow, small turbulent eddies being swept down stream or the passage of trailing tip vortices of a previous blade passage.

When they occur near the onset or recovery of stall, they may indicate the progression of flow separation across the blade. As such the disturbances may be related to the "separation vortex" moving aft and "moment stall"².

Disturbances were not detected sweeping from the leading edge all the way across to the trailing edge except for possibly one case. If this had been observed generally, it might have been an indication of that vortex shedding from the leading edge could trigger a complete flow separation. Disturbances were only rarely seen to sweep from the leading edge to the trailing edge. Figures 9 and 13 give an indication of a progressive disturbance. Such observations may be indications that vortex shedding from the leading edge could progress aft and trigger complete flow separation. Such phenomena were not generally observed, however.

6.2 Specific Trace Evaluation

Study of the traces of the bottom graph in Figure 8, indicates quite clearly that separation is initiated at about 290° for the 71% chord trace followed by separation at about 310° for the 54% trace. Recovery from "stall" seems to take place sooner for the 54% trace, at 40° azimuth, than for the 71% trace at 50°. A study of both graphs reveals that trailing edge separation occurs without any noticeable effect on the 10 or 24% chord traces.

If one considers figure 9, with $\theta = 10^\circ$, $\mu = 0.16$, and 5° shaft tilt an interesting stall propagation can be observed in the upper figure. A leading edge disturbance at 10% chord is first seen at 225° azimuth which appears a short time later in the 24% trace. The 10% trace shows the start of oscillation, probably some type of leading stall phenomena, at ~ 250°. The 24%

trace shows the start of a similar disturbance about 1/4 of a timing trace division (~ 0.0025 s) later. In both traces the disturbance lasts until about 330° with the leading edge, 10% chord trace recovering about 0.003 second after the 24% trace. This action indicates that the leading edge experiences "stall" before the quarter chord and recovers after the quarter chord. In this upper figure the trailing edge (71% chord) separation which appears evident extends from 240° to 40° . The trailing edge action seems independent of the leading edge action.

If we now view the lower half of figure 9 and examine the 54 and 71% traces, it seems quite evident that the midchord separation action initiates after and recovers before the 71% chord. It is also possible to trace a disturbance which seems to occur at 290° for the 10% chord, to a more severe oscillation at a similar azimuth with the 54% trace, and also to a sudden change at the 71% chord. This action does possibly indicate either a boundary layer disturbance propagating rearward, or the influence of external flow action. It does appear that whatever the source, the action moves aft and increases the severity of separation at the 71% chord.

If figure 17 with $\theta = 15^\circ$, $\mu = 0.24$, and 5° shaft tilt is studied, it can be seen from the bottom graph that in the region of 30° to 90° azimuth an oscillation exists in both the 54 and 71% traces. The oscillations are approximately in phase and seem to be related. It is tempting to hypothesize that the oscillation is due to blade torsion affects as often suggested in the case of full scale rotor blade pitching oscillations following stall. However, two factors mitigate against such a conclusion. First the test blade is extremely stiff in torsion with a relatively low aspect ratio. It is mounted directly to the rotor hub with no cyclic or collective pitch system. Blade pitch change is accomplished by a bolted attachment at the root of the blade. Hence it is doubtful that the oscillation of the traces is due to blade oscillation. Secondly, examination of the 10% chord trace in the same graph does not reveal a similar oscillation. If blade pitch oscillation would occur, then all blade traces would exhibit similar oscillations. Rear trace oscillations in the same azimuth regions can also be seen in other test conditions, as evidenced in figures 14, 15, 16, 18, and 19.

If one considers the effect of increasing the pitch angle, θ , at the higher advance ratios, it is evident that separation and boundary layer disturbances increase in amount and magnitude of azimuth at the higher pitch angles. For a tilt of 5° , and $\mu = 0.16$, as θ is increased from $\theta = 5^\circ$ to $\theta = 10^\circ$ to $\theta = 15^\circ$, the severity of trailing edge separation increases (figures 3, 19, and 15). The leading edge shows no indication of oscillation at $\theta = 5^\circ$, but at $\theta = 10^\circ$ some oscillation seems to occur and at 15° full separation is evident.

For the case of tilt of 5° and $\mu = 0.24$ (figures 15, 11, and 17) the leading edge shows little evidence of stall at $\theta = 5^\circ$, with some significant oscillation at $\theta = 10^\circ$ in the azimuth range of 280° to 340° . Trailing edge separation is evident at all pitch angles, but the severity of the stall has increased and the azimuth range increased for $\theta = 10^\circ$ over that for $\theta = 5^\circ$. At $\theta = 15^\circ$ massive amounts of stall exist over the entire chord from 200° azimuth to about 10° azimuth.

For the case of tilt of 5° and $\mu = 0.32$ (figures 7, 13, and 19) it is apparent that at $\theta = 5^\circ$ little leading edge action is taking place, but some disturbance exists after 220° azimuth at $\theta = 10^\circ$, and that full separation exists at $\theta = 15^\circ$ over 200° to 10° azimuth. Trailing edge separation exists at $\theta = 5^\circ$, and the severity increases until at $\theta = 15^\circ$ the separation exists

for the entire azimuth except for a region of about 90° to 180° .

These same results can be seen from Figures 21-24 where the azimuthal positions where separation initiates and terminates are depicted. These figures show the influence of advance ratio at fixed blade pitch angle and for a tilt angle of 5° . It must be recognized that it is quite difficult to fix the position of separation and reattachment with certainty. Particularly in the aft portion of the blade chord the velocity decreases so gradually in many cases that it is difficult to precisely determine the azimuth where separation begins or ends. Figures 25-28 indicate similar separation regions for a tilt angle of $\alpha = -10^\circ$.

Thus, as one would expect, as θ is increased for a given advance ratio the separation and stall phenomena increase in magnitude and severity. If one considers the same data as advance ratio is increased for a fixed θ , similar trends are seen, but for the cases considered the effect is not quite as dramatic.

For fixed θ and advance ratio, changing shaft tilt from 5° to 10° does not seem to have a marked influence on the nature of the traces either at the leading edge or elsewhere on the chord.

A comparison with the hot film surface gage data of reference 5 reveals that whereas those results indicate evidence of leading edge separation in all cases where trailing edge separation phenomena are shown, the data of figures 21 and 24, and 25 and 28 show that trailing edge separation occurs independently of leading edge except at the highest pitch angle. The difference may arise because of Reynolds number, however since no Reynolds numbers are given in reference 5, no conclusive statement may be made.

Further details on the work presented herein may be found in reference 6.

7. CONCLUSIONS

1. Separation occurs near the trailing edge for blade pitch angles of 5° or more and advance ratios of 0.16 or more. The separation gradually moves toward the leading edge at stall onset, and then back again during recovery. This is typical of trailing edge stall.
2. During trailing edge stall the separation seems to move across the blade at velocities ranging from about 3 to 9% of the theoretical free-stream velocity.
3. For blade pitch angles of 15° and advance ratios greater than 0.16, separation occurs near the leading edge as well as at the trailing edge. The leading edge separation is very abrupt, and it appears to be a separate phenomenon from trailing edge stall. At pitch angles of 10° and the higher advance ratios, some evidence of leading edge action is observed.
4. When stall occurs near the leading edge it rapidly sweeps rearward across the blade at a velocity approaching the theoretical free stream velocity. Since this suggests the bursting of a small laminar separation bubble, the stall may be a form of leading edge stall.

5. Using hot wire anemometers, small disturbances in the flow other than the separation affects can sometimes be traced as they propagate downstream. They sweep across the blade at velocities ranging from about 30 to 100% of the free stream velocity.

REFERENCES

1. Lachmann, G.V., Boundary Layer and Flow Control, Pergamon Press, New York, 1961.
2. McCroskey, W.J., Fisher, R.K., "Detailed Aerodynamic Measurements on a Model Rotor in the Blade Stall Regime", J. Am. Helicopter Soc., Vol. 6, No. 1, 1972.
3. Velkoff, H.R., Hoffman, J.D., Blaser, D.A., "Investigation of Boundary Layers and Tip Flows of Helicopter Rotor Blades", USAAVLABS Technical Report 71-73, U.S. Army Aviation Material Laboratories, Fort Eustis, Virginia, May 1972.
4. Velkoff, H.R., Blaser, D.A., Shumaker, G.C., Jones, K.M., "Exploratory Study of the Nature of Helicopter Rotor Blade Boundary Layers", USAAVLABS Technical Report 69-50, U.S. Army Aviation Material Laboratories Fort Eustis, Virginia, July 1969.
5. Philippe, J., Armand, C., "ONERA Research Work on Helicopters", AGARD Symposium on Rotorcraft Design, NASA Ames Research Center, May 16-19, 1977.
6. Ghai, R.L. and Velkoff, H.R., "A Study of Stall and Separation on the Retreating Blade of a Helicopter Rotor Using Hot Wires", Ohio State University Research Foundation Report, RF783375, Vol. II and NASA Ames Research Center, Moffett Field, California 94035, Contract NAS-2-6779, April 1978.

LIST OF SYMBOLS

C_L	Lift coefficient
Re	Reynolds number
U	Free stream velocity
Ψ	Azimuth angle of blade
μ	Advance ratio
θ	Blade pitch angle

* This work was sponsored by the U.S. Army Research and Technology Aeromechanics Laboratory, Ames Research Center, California.

15-11

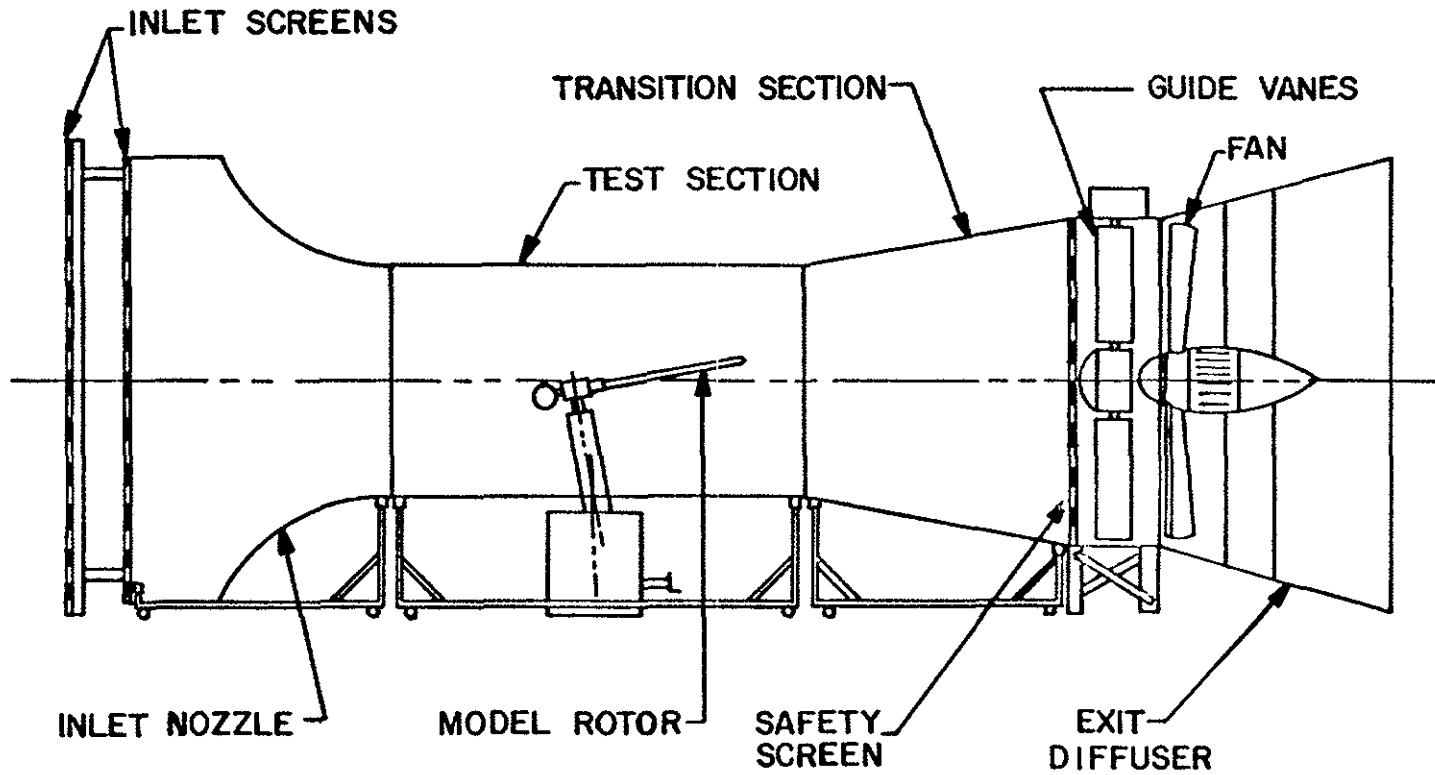


Figure 1. Model Rotor Wind Tunnel

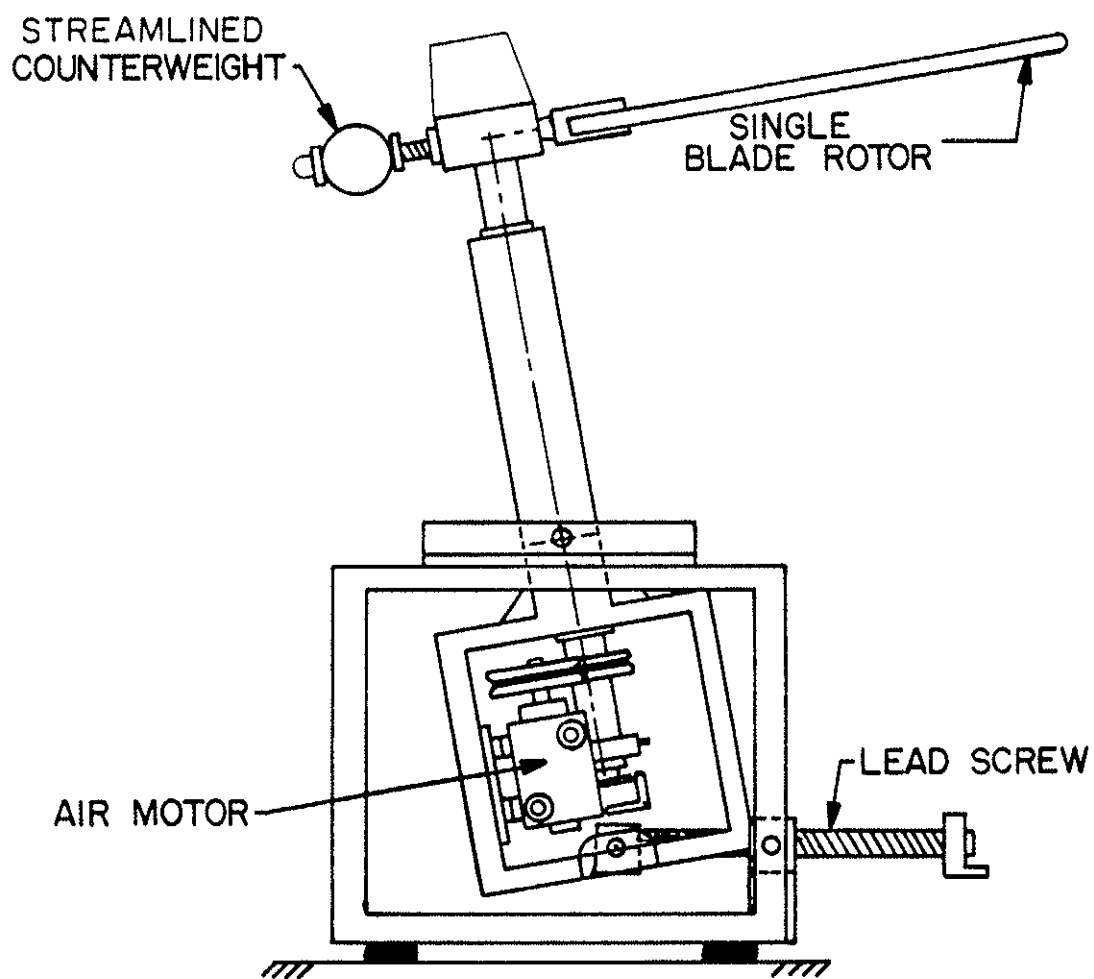


Figure 2. Rotor Drive System for Forward Flight Tests

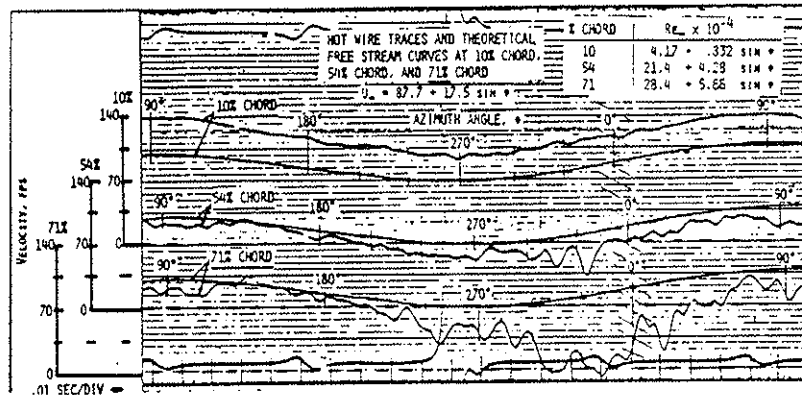
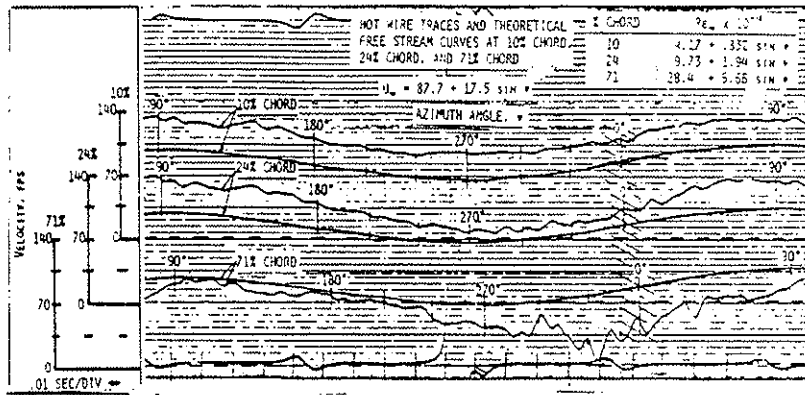


Figure 3. Data at 5° Blade Pitch, 0.16 Advance Ratio, and 5° Shaft Angle

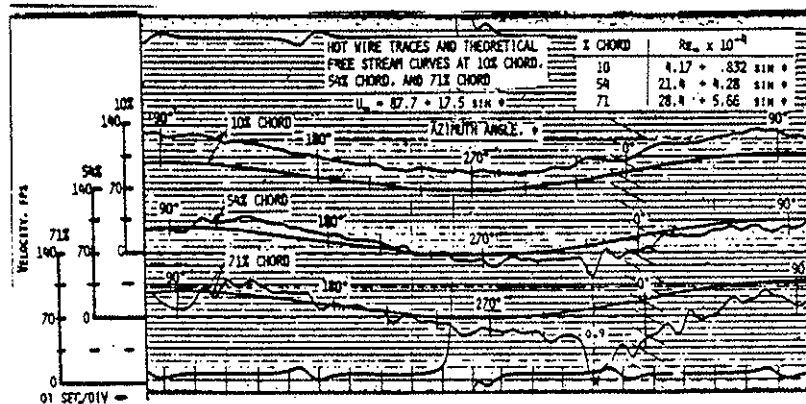
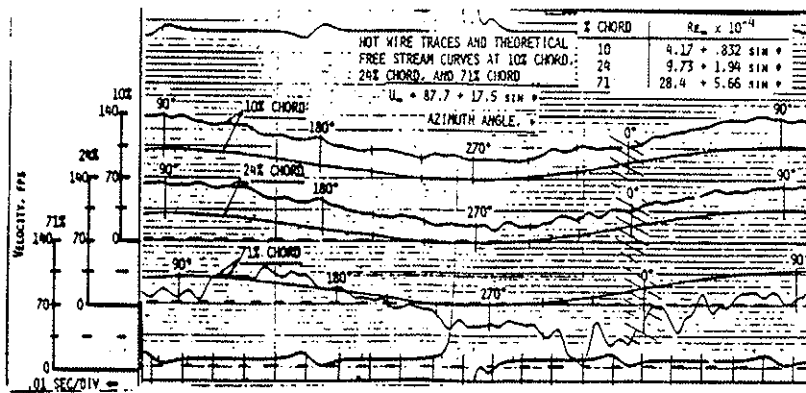


Figure 4. Data at 5° Blade Pitch, 0.16 Advance Ratio and 10° Shaft Angle

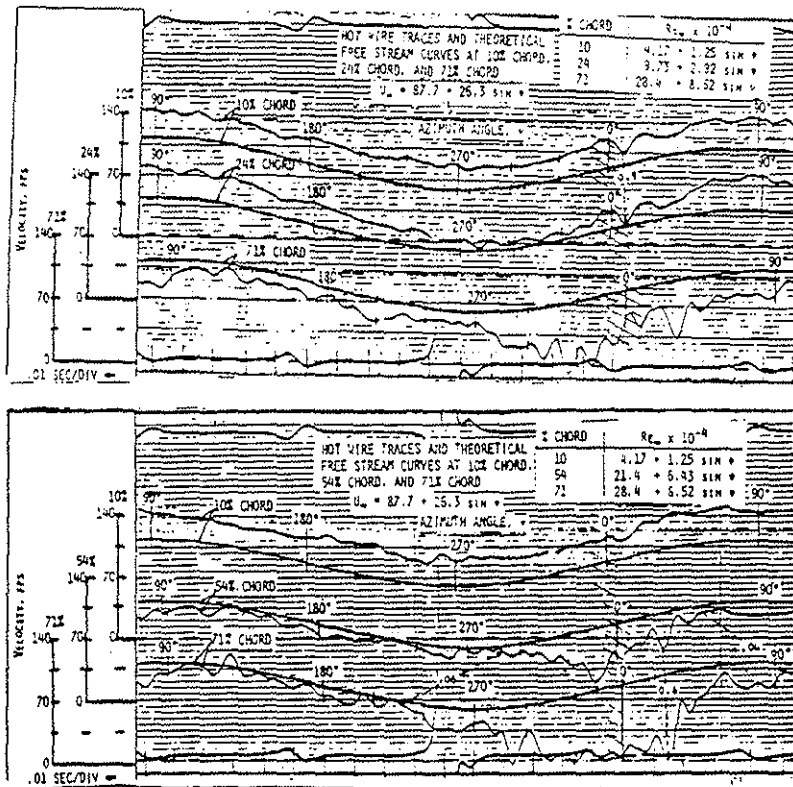


Figure 5. Data at 5° Blade Pitch, 0.24 Advance Ratio, and 5° Shaft Angle

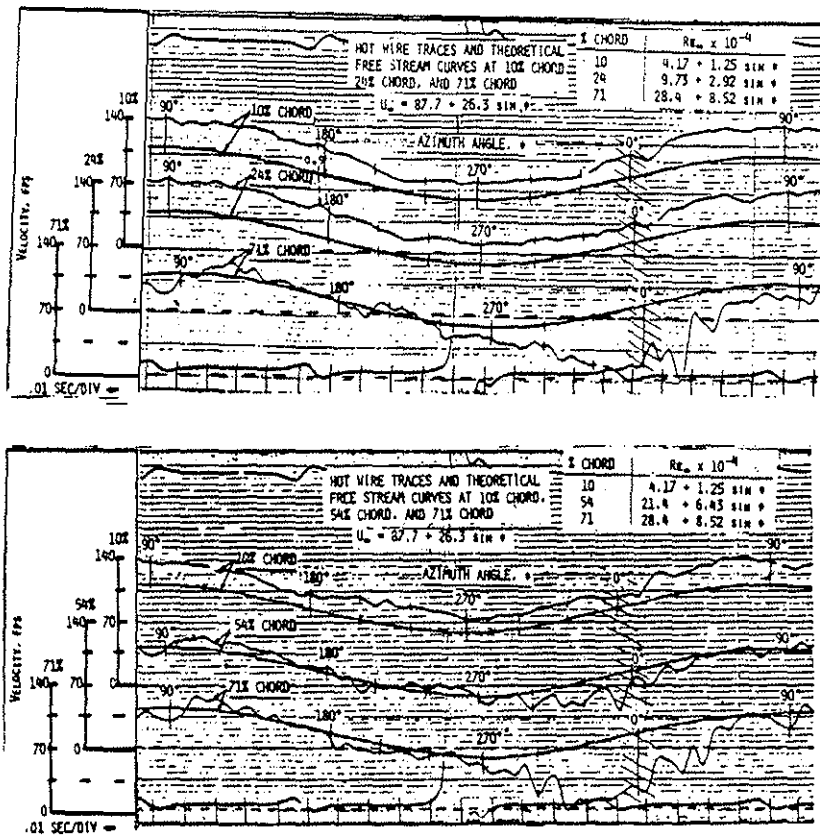


Figure 6. Data at 5° Blade Pitch, 0.24 Advance Ratio, and 10° Shaft Angle

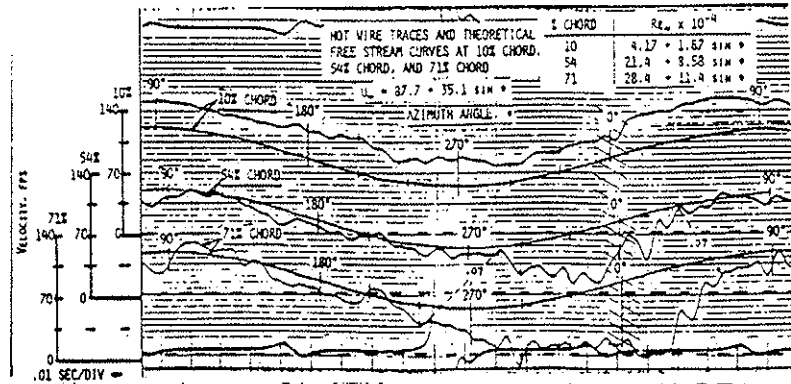
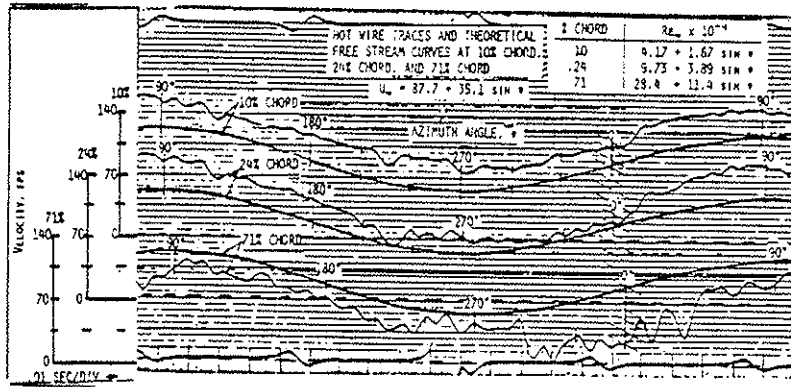


Figure 7. Data at 5° Blade Pitch, 0.32 Advance Ratio, and 5° Shaft Angle

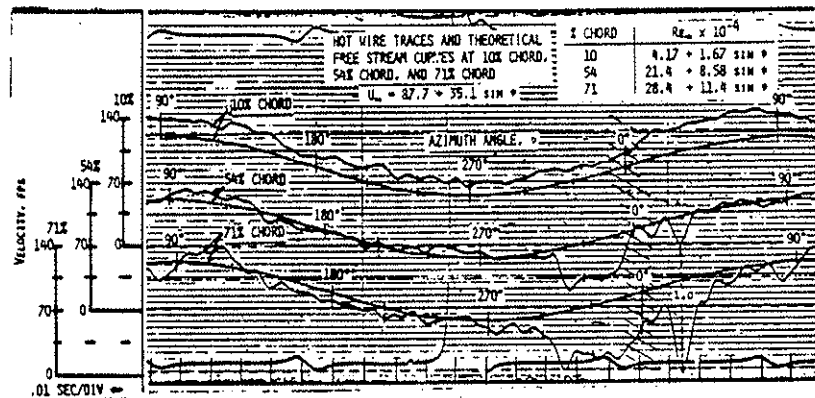
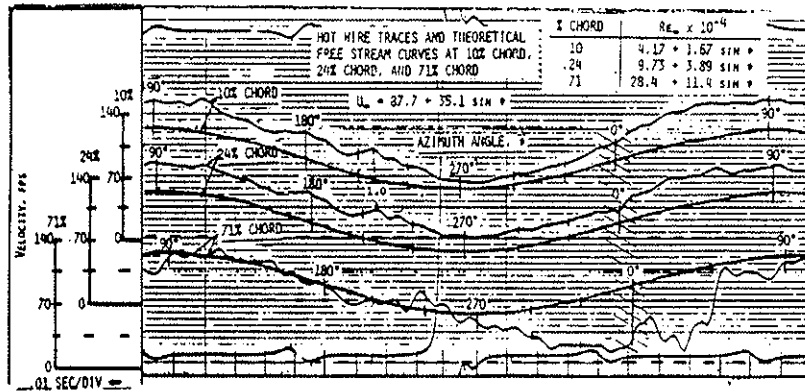


Figure 8. Data at 5° Blade Pitch, 0.32 Advance Ratio, and 10° Shaft Angle

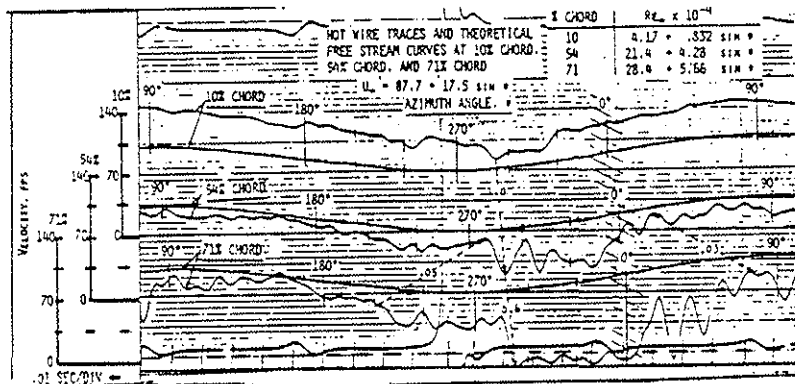
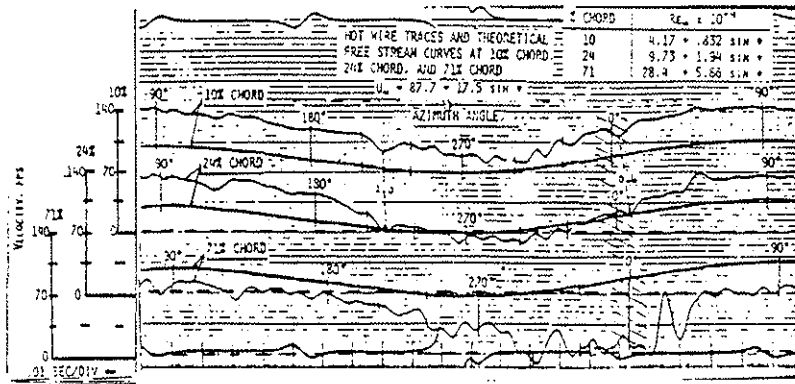


Figure 9. Data at 10° Blade Pitch, 0.16 Advance Ratio, and 5° Shaft Angle

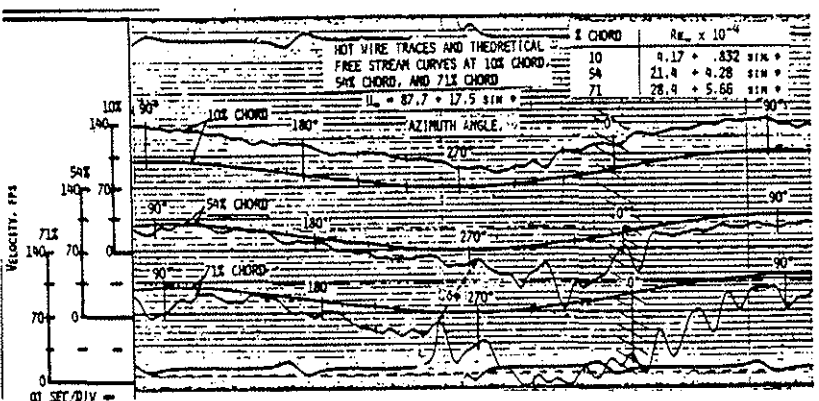
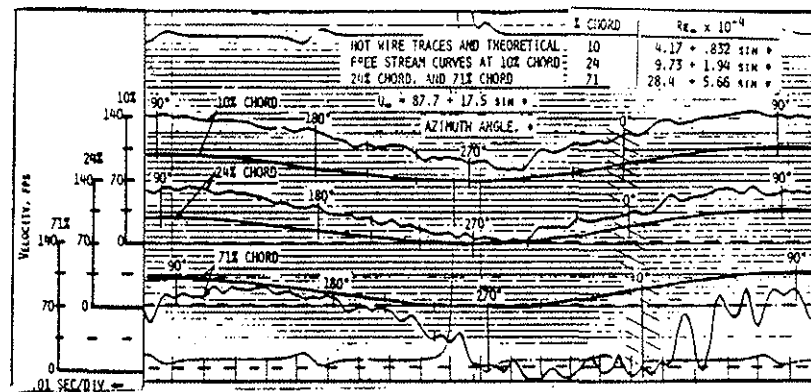


Figure 10. Data at 10° Blade Pitch, 0.16 Advance Ratio, and 10° Shaft Angle

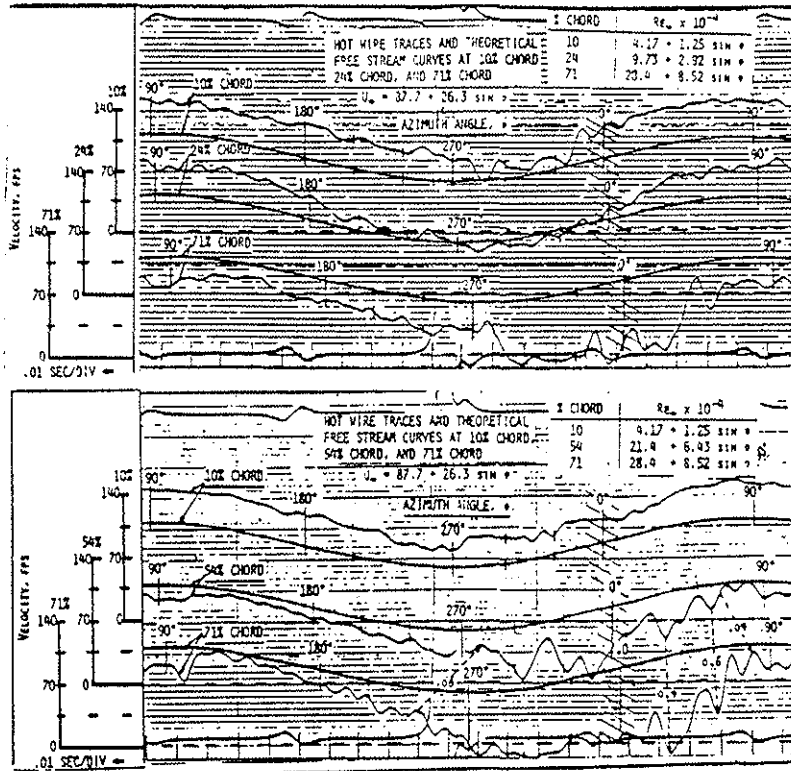


Figure 11. Data at 10° Blade Pitch, 0.24 Advance Ratio, and 5° Shaft Angle

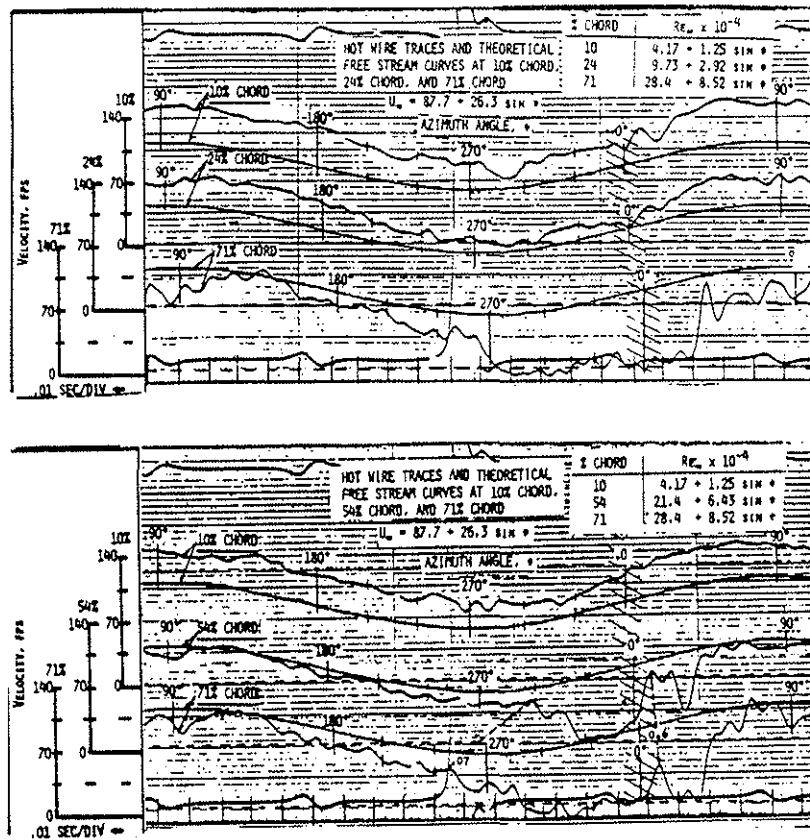


Figure 12. Data at 10° Blade Pitch, 0.24 Advance Ratio, and 10° Shaft Angle

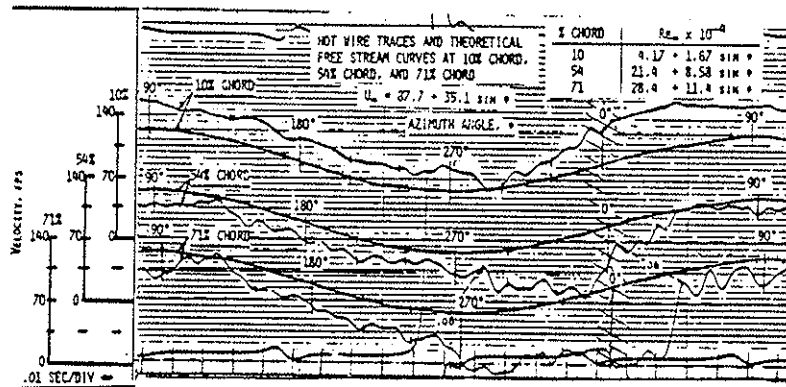
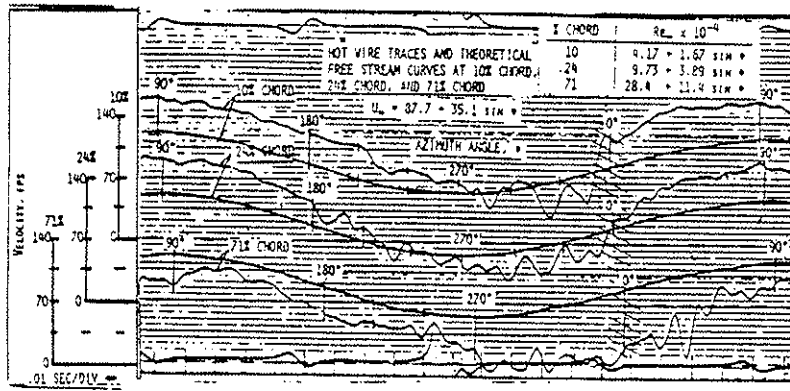


Figure 13. Data at 10° Blade Pitch, 0.32 Advance Ratio, and 5° Shaft Angle

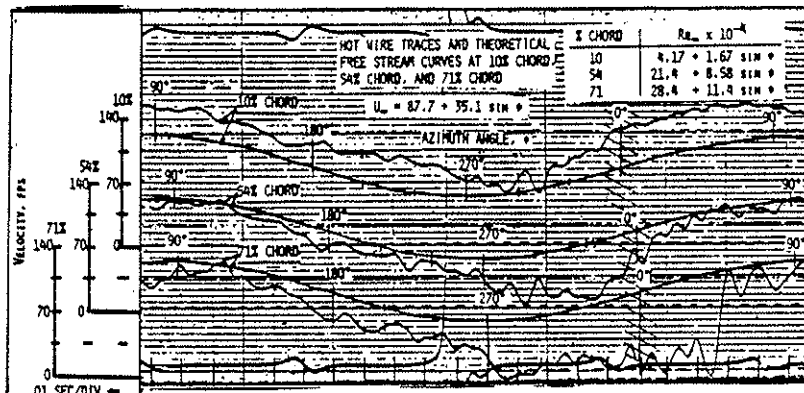
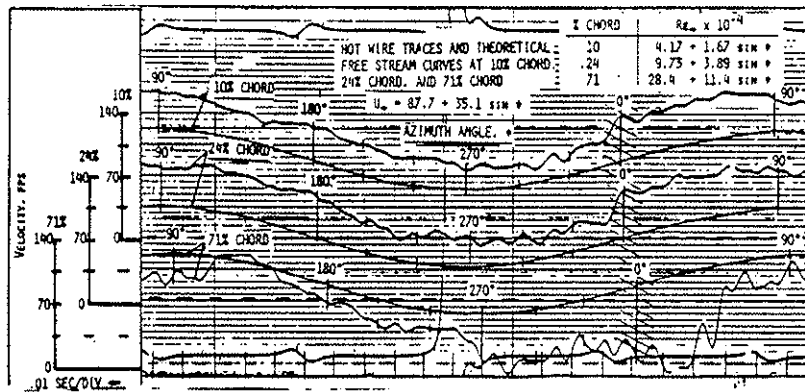


Figure 14. Data at 10° Blade Pitch, 0.32 Advance Ratio, and 10° Shaft Angle

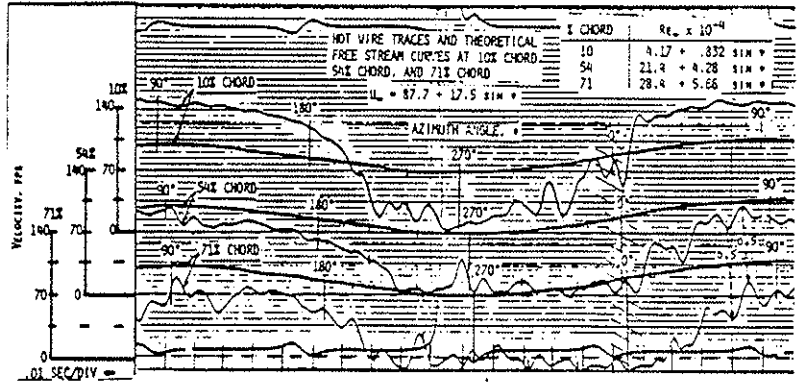
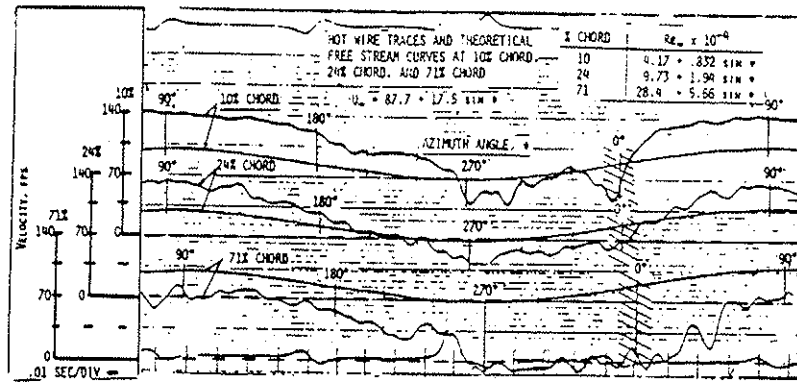


Figure 15. Data at 15° Blade Pitch, 0.16 Advance Ratio, and 5° Shaft Angle

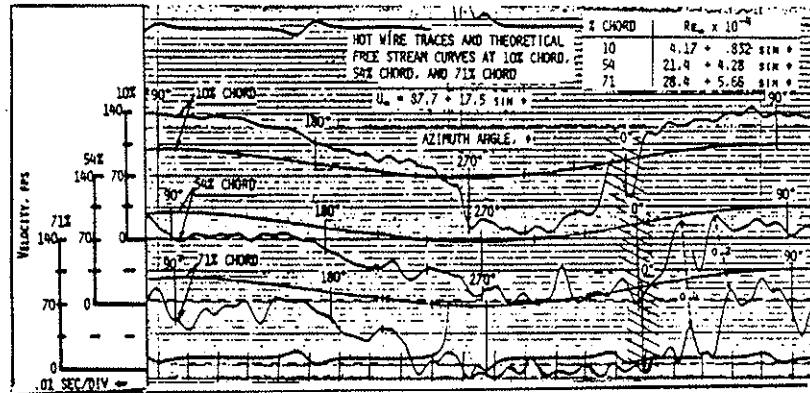
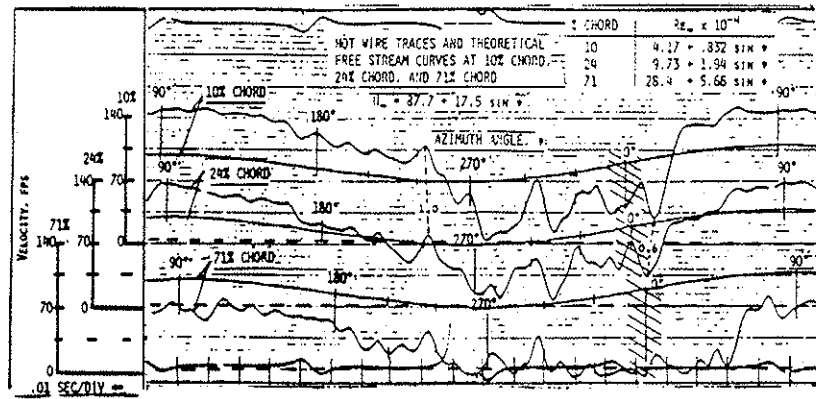


Figure 16. Data at 15° Blade Pitch, 0.16 Advance Ratio, and 10° Shaft Angle

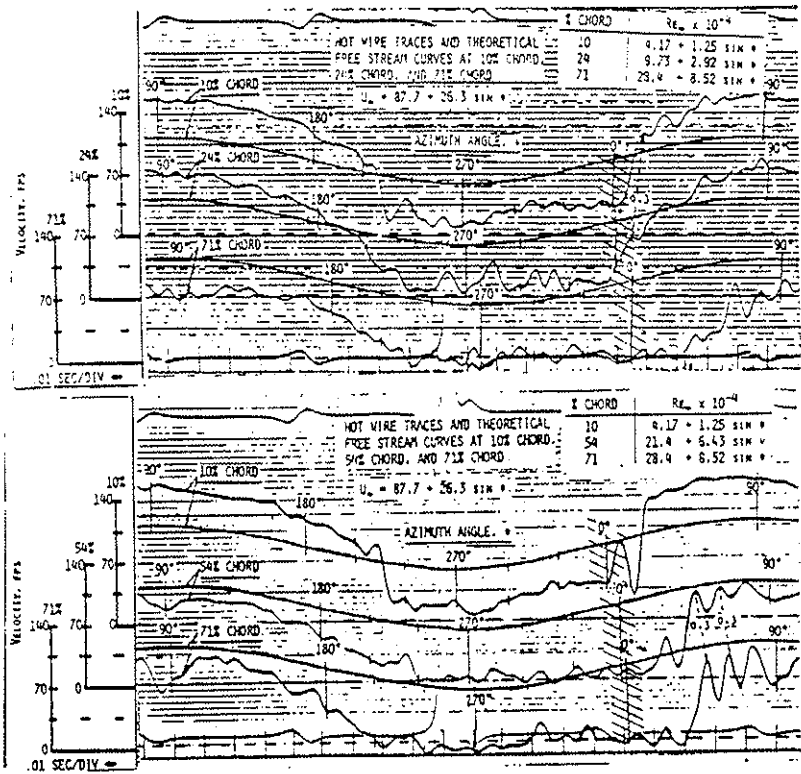


Figure 17. Data at 15° Blade Pitch, 0.24 Advance Ratio, and 5° Shaft Angle

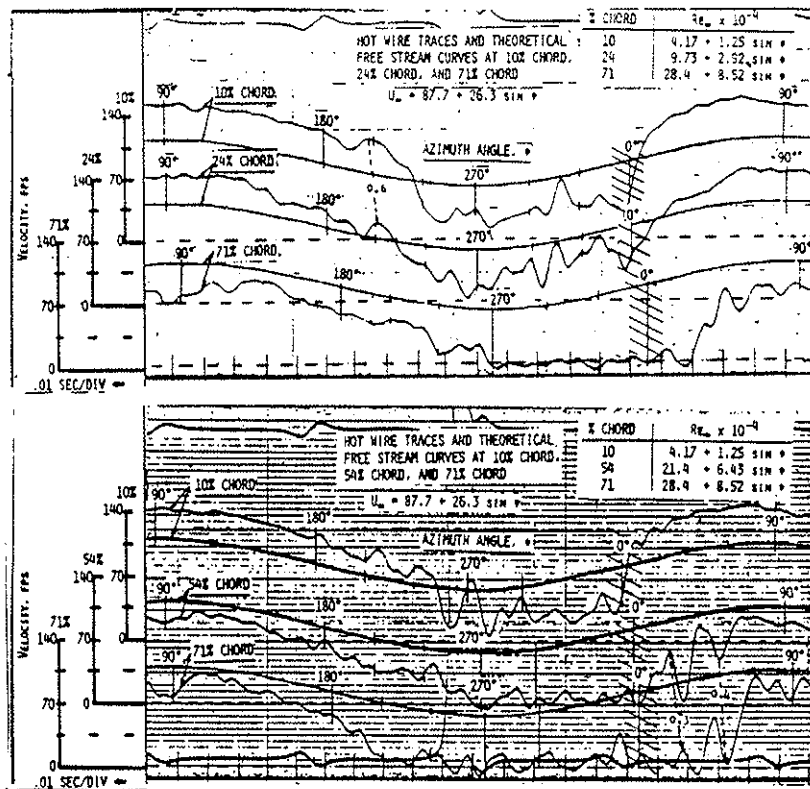


Figure 18. Data at 15° Blade Pitch, 0.24 Advance Ratio, and 10° Shaft Angle

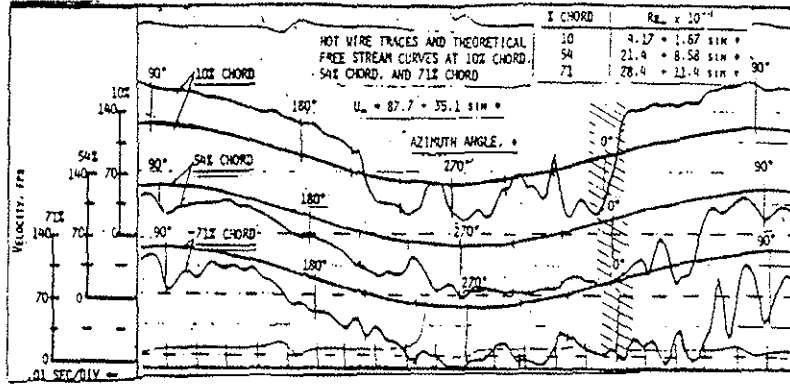
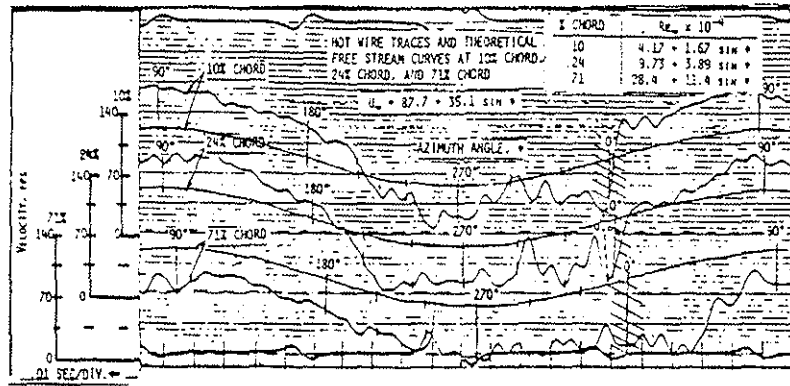


Figure 19. Data at 15° Blade Pitch, 0.32 Advance Ratio, and 5° Shaft Angle

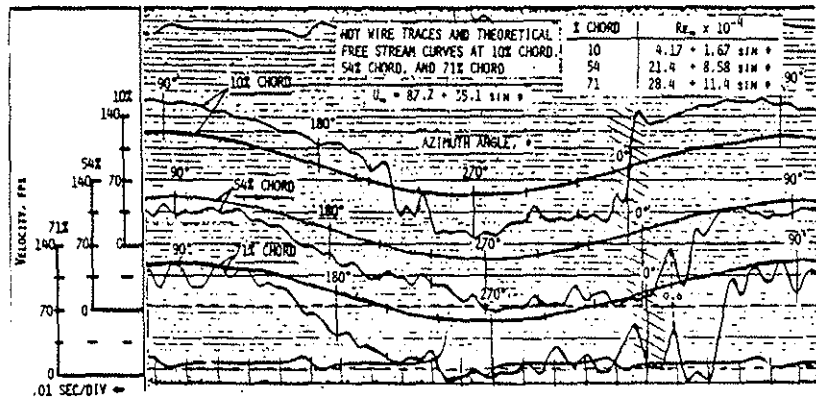
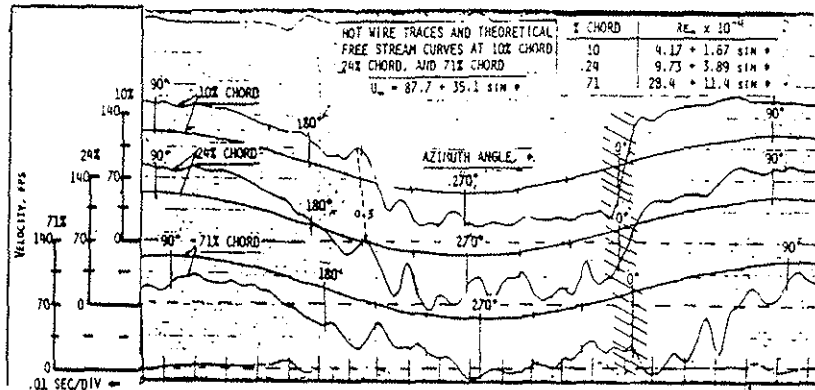


Figure 20. Data at 15° Blade Pitch, 0.32 Advance Ratio and 10° Shaft Angle

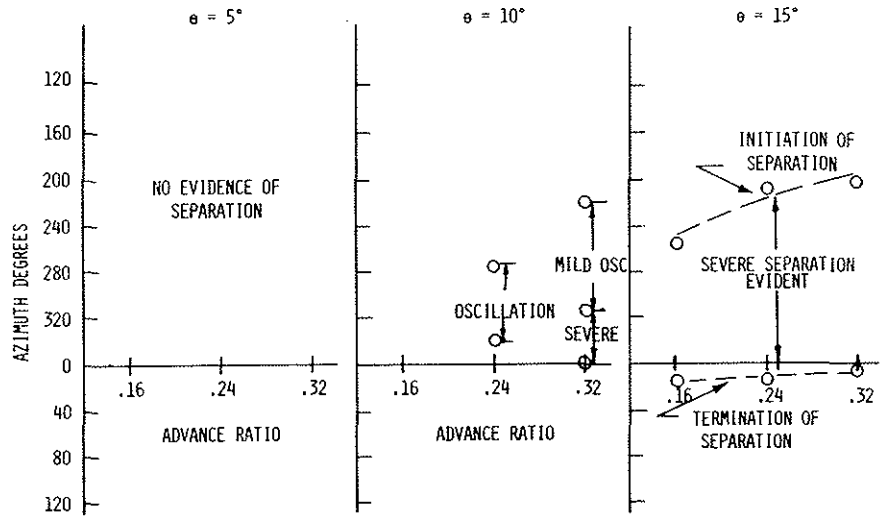


Figure 21. Azimuthal positions where separation initiates and terminates. Shaft tilt $\alpha = -5^\circ$, 10% chord position, $r/R = 0.8$

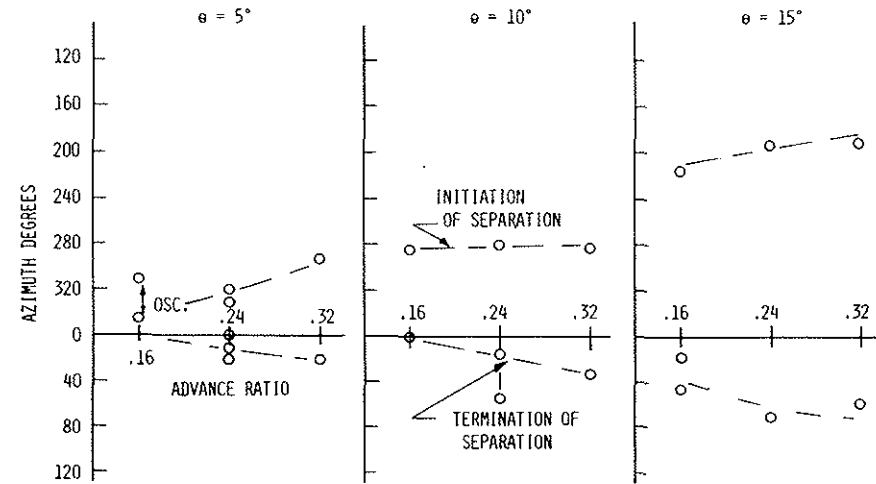


Figure 23. Azimuthal positions where separation initiates and terminates. Shaft tilt $\alpha = -5^\circ$, 54% chord position, $r/R = 0.8$

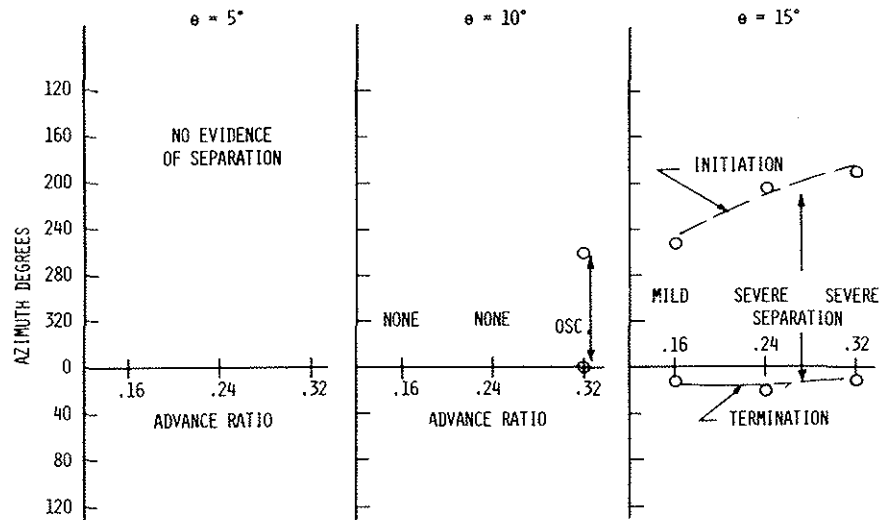


Figure 22. Azimuthal positions where separation initiates and terminates. Shaft tilt $\alpha = -5^\circ$, 24% chord position, $r/R = 0.8$

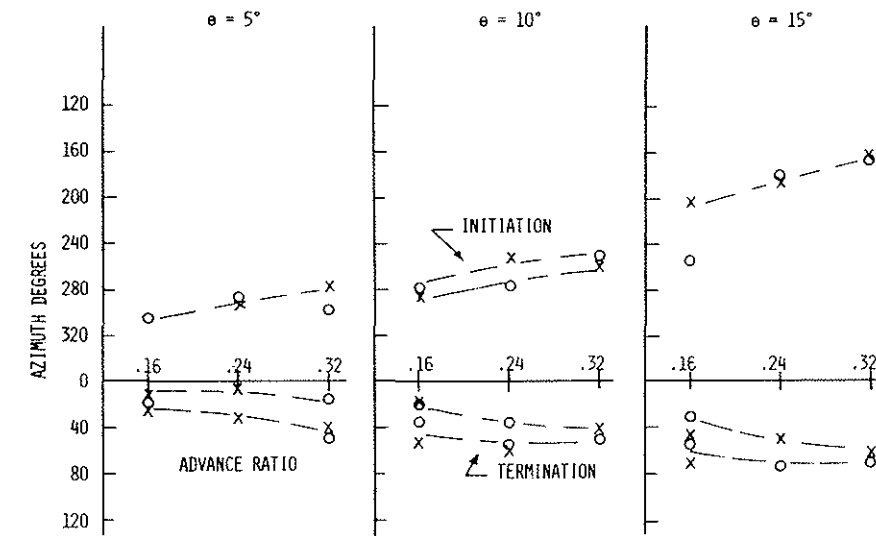


Figure 24. Azimuthal positions where separation initiates and terminates. Shaft tilt $\alpha = -5^\circ$, 71% chord position, $r/R = 0.8$



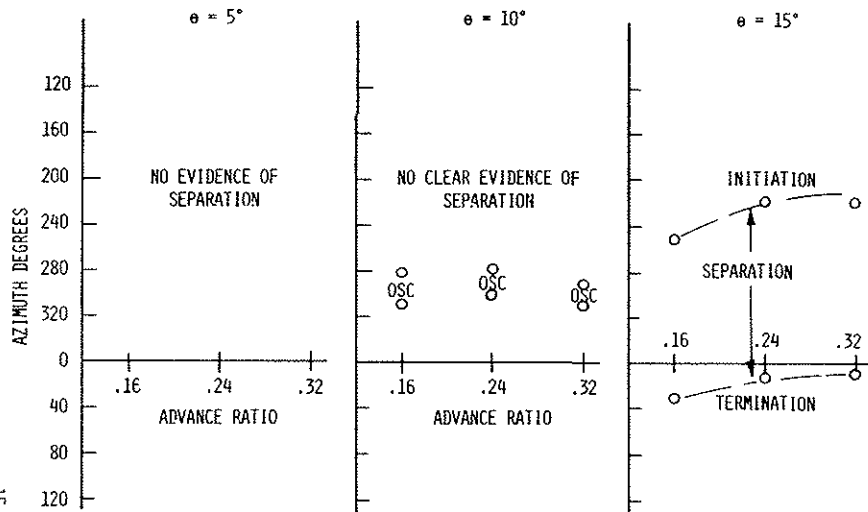


Figure 25. Azimuthal positions where separation initiates and terminates. Shaft tilt $\alpha = -10^\circ$, 10% chord position, $r/R = 0.8$

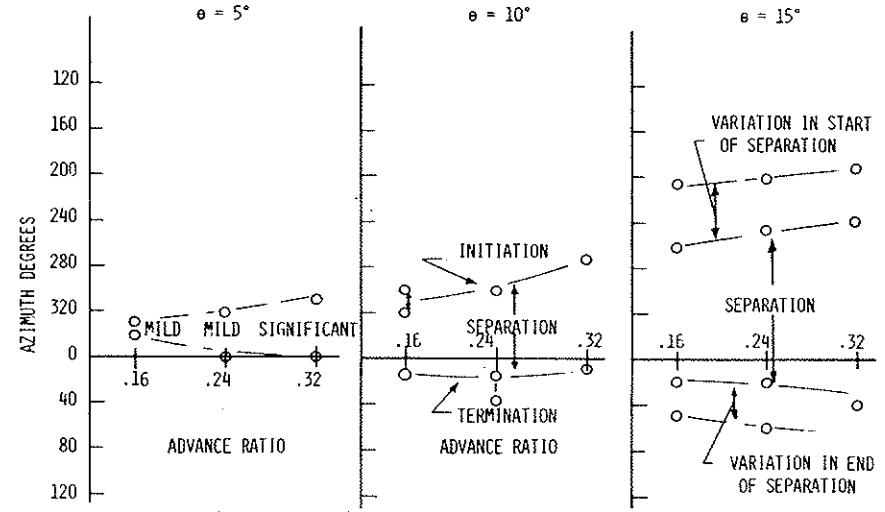


Figure 27. Azimuthal positions where separation initiates and terminates. Shaft tilt $\alpha = -10^\circ$, 54% chord position, $r/R = 0.8$

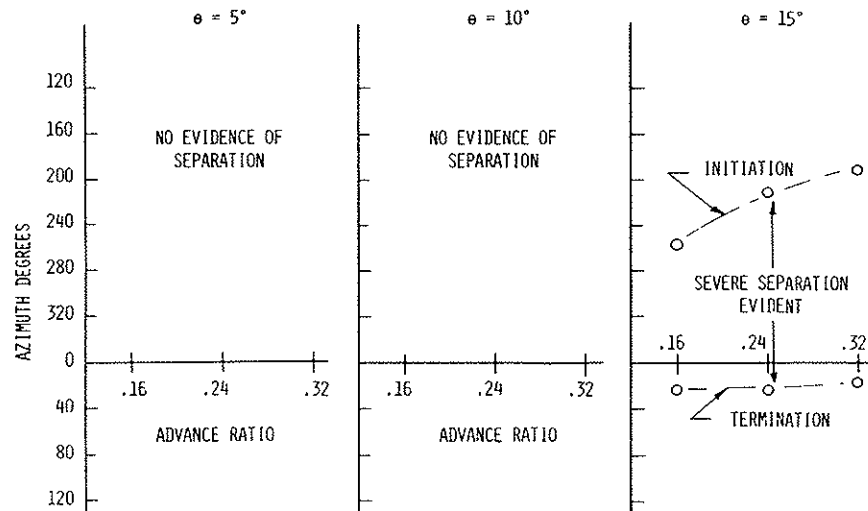


Figure 26. Azimuthal positions where separation initiates and terminates. Shaft tilt $\alpha = -10^\circ$, 24% chord position, $r/R = 0.8$

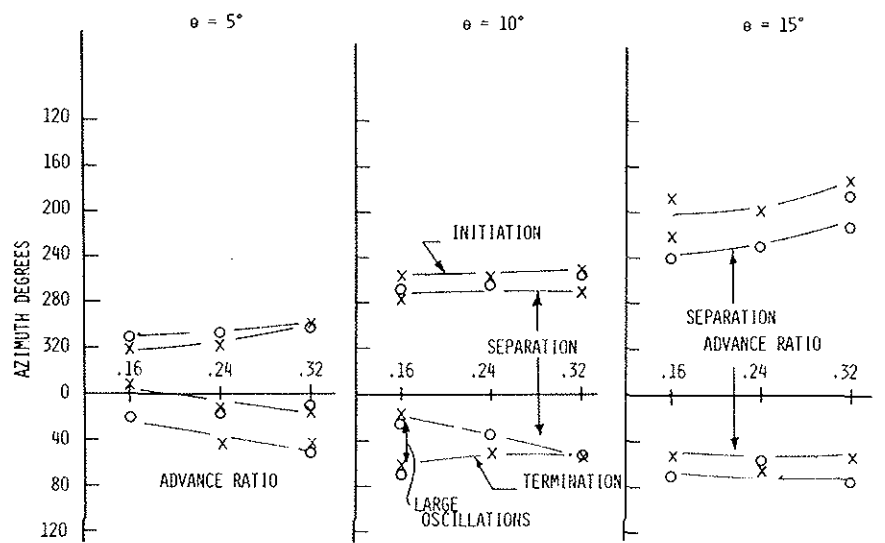


Figure 28. Azimuthal positions where separation initiates and terminates. Shaft tilt $\alpha = -10^\circ$, 71% chord position, $r/R = 0.8$